

Synthesis and in Vivo Evaluation of New Contrast Agents for Cardiac MRI

Nada H. Saab-Ismail, Tamás Simor, Balázs Gaszner, Tamás Lóránd, Márta Szöllösy, and Gabriel A. Elgavish*

Department of Biochemistry and Molecular Genetics, University of Alabama at Birmingham, Birmingham, Alabama 35294

Received August 4, 1998

Analogues 2–6 of N^3, N^6 -bis(2'-myristoyloxyethyl)-1,8-dioxotriethylenetetraamine- N, N, N, N' -tetraacetic acid (BME-DTTA) (1), which like 1 are also based on the DTTA structure but contain shorter fatty acyl chains, were synthesized to improve the water solubility of the corresponding gadolinium complexes. The gadolinium complexes of 1 and 3–5 have very low solubility in water. Thus liposomal preparations are necessary for their in vivo MRI application. These liposomal preparations retain high in vitro relaxivities (27.1, 21.57, 20.32, 23.1 s⁻¹ mM⁻¹, respectively) and induce sustained MRI signal intensity enhancements (67.2, 38.4, 52.1, 41.7 in arbitrary units, respectively). The gadolinium complex of 2 is quite soluble in water. Its lifetime in the blood stream, however, is short. The gadolinium complex of analogue 6, N -(2-butyryloxyethyl)- N' -(2-ethyloxyethyl)- N, N' -bis[N'', N'' -bis(carboxymethyl)acetamidol]-1,2-ethanediamine (ABE-DTTA), has demonstrated its potential as a water-soluble, cardiac-specific, MRI contrast agent. It is completely soluble in water at a 25 mM concentration, allowing the preparation of an injectable dose. The in vitro relaxivity of the complex is 16.24 s⁻¹ mM⁻¹. The agent shows a specific accumulation in the heart tissue reaching its maximum within 15 min after administration, inducing a sustained MRI signal intensity enhancement of 43.6%. This enhancement lasts for at least 3 h, thus indicating a reasonably long lifetime of this contrast agent in the myocardium without deleterious effects on heart function parameters.

Introduction

Much attention has been focused on the development of a noninvasive method for early detection of coronary heart disease. Coronary heart disease is the main cause of death in western societies,¹ and thus, early institution of effective medical or surgical therapy would be highly desirable. Such early therapy requires a reliable method of early diagnosis. Among existing methods, magnetic resonance imaging (MRI) is the most promising.^{2–4} In addition to its superb diagnostic characteristics, MRI is also devoid of most problems inherent in the currently used Tl-201 radionuclide myocardial imaging technique such as low spatial resolution, tissue attenuation, scatter, lack of ease of quantitation and of tomographic evaluation, and other technical problems.⁵ In addition, MRI is safe and lacks the biological hazards associated with other techniques such as X-ray and radionuclide imaging.⁶

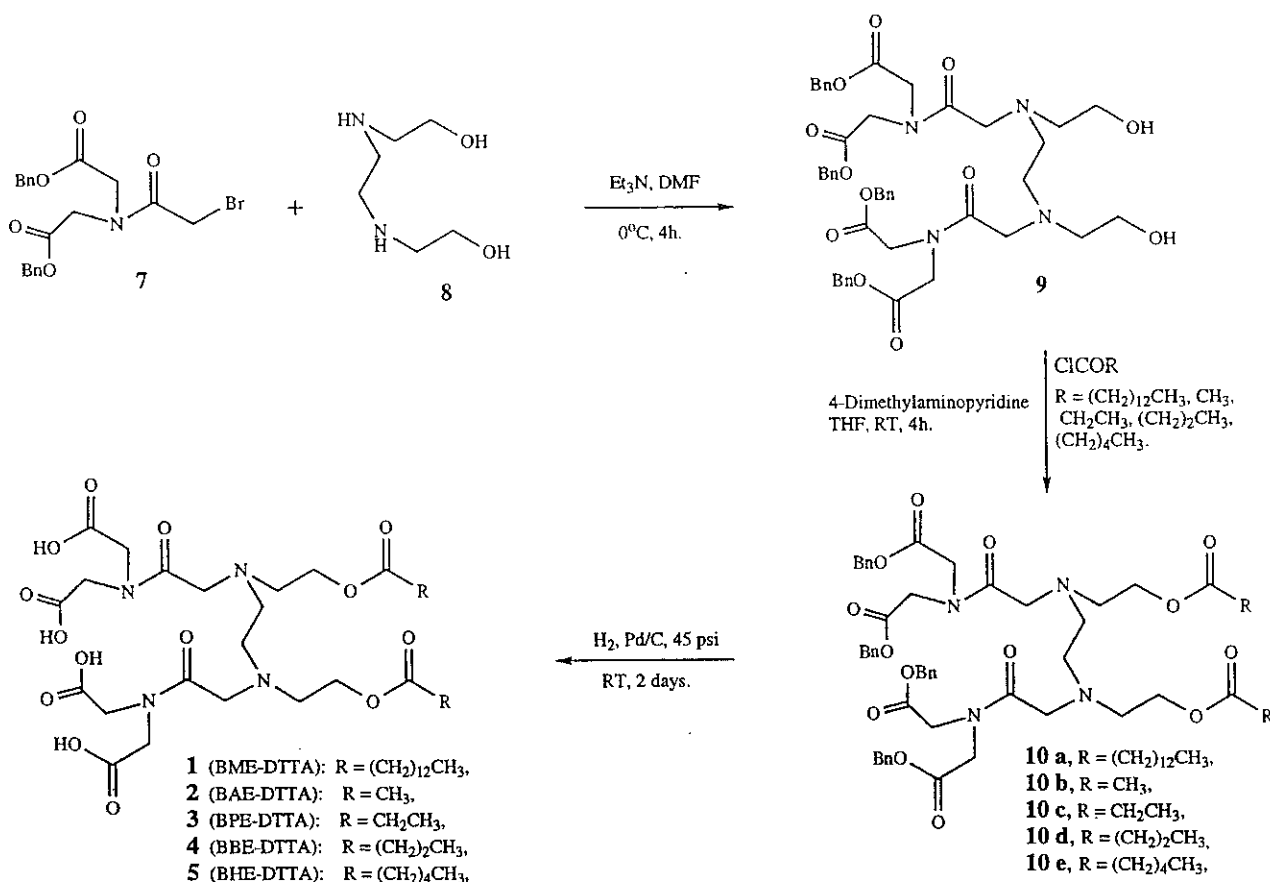
In principle, MRI provides three-dimensional, high-resolution images of protons, mainly of water molecules. The MRI signal intensity is largely determined by proton relaxation rates and is most useful when based on differences in the relaxation rates, $1/T_1$ (longitudinal) and $1/T_2$ (transverse), tissue contrasts of great diagnostic value are obtained. Unfortunately, however, although MRI offers excellent soft tissue resolution, it is hampered by the lack of sufficient signal contrast between underperfused and well-perfused myocardium. Thus, acute myocardial ischemia cannot be detected without the induction of relaxation rate differences

between normal versus ischemic tissue. Therefore, contrast agent-enhanced MRI is currently the main technique with the potential to enable early detection of acute myocardial ischemia.⁷ Contrast agents that distribute in the myocardium in proportion to the level of perfusion can create relaxation rate differences, thus effecting functional enhancement of contrast in MRI images. Existing agents, however, are neither sufficiently tissue specific nor retained long enough in the myocardium to allow stress-coupled MRI of perfusion.

The relaxation rates of water protons can be enhanced by interaction with paramagnetic moieties which are organic molecules or metal ions that carry unpaired electrons. Among the paramagnetic lanthanide metal ions, the S-state gadolinium (Gd^{3+}) induces the largest relaxation enhancement.^{8,9} Free lanthanide aquo ions, however, have limited solubility at physiological pH. In addition, these lanthanide ions are highly toxic due to their tendency to inhibit various biochemical processes, most probably by replacing calcium.¹⁰ Organic chelators that bear the negatively charged carboxylate groups have the ability to form strong complexes with Gd^{3+} , forming nontoxic contrast agents for proton MRI. These agents typically retain between one and three water molecules in the inner coordination sphere of Gd^{3+} , enabling water proton relaxation rate enhancement through fast exchange of the bound water molecules with the free bulk water molecules. Ionic complexes such as gadolinium diethylenetriaminepentaacetic acid ($Gd[DTPA(H_2O)]^{2-}$)^{11,12} and gadolinium 1,4,7,10-tetraazacyclododecane- N, N', N'', N''' -tetraacetic acid ($Gd[DOTA-(H_2O)]^{1-}$)^{12,13} and neutral complexes such as gadolinium diethylenetriaminepentaacetic acid bismethylamide ($Gd[DTPA-BMA(H_2O)]$)¹⁴ and gadolinium 10-(2-hydroxypropyl)-1,4,7,10-tetraazacyclododecane-1,4,7-triacetic acid

* To whom correspondence should be addressed: Department of Biochemistry and Molecular Genetics, Rm 336, Tinsley Harrison Tower, 1900 University Blvd, University of Alabama at Birmingham, Birmingham, AL 35294-0006. Tel: (205) 934-0294. Fax: (205) 934-0031. E-mail: gabi@uab.edu.

Scheme 1



(Gd[HP-DO3A(H₂O)])¹⁵ are contrast agent complexes currently in general use. Recent search for new, specific contrast agents has been directed toward the synthesis of Gd³⁺ complexes of functionalized derivatives of DTPA and DOTA without altering their chelating ability. Their water proton relaxivity is increased by conjugating them to macromolecules such as albumin-DTPA¹⁸ or by modification of the basic structure of the chelate such as in gadolinium (1*R*,4*R*,7*R*)- α,α',α'' -trimethyl-1,4,7,10-tetraazacyclododecane-1,4,7-triacetic acid (Gd[DO3MA-(H₂O)]).¹⁹ They have, however, a short residence time in the blood stream and in tissue and are nonspecific to myocardial tissue. Consequently, these agents have a limited usefulness for the detection of acute myocardial ischemia.^{7,16,17}

Targeting of a contrast agent to a particular site within the body is currently a developing challenge. To address the myocardial specificity issue, fatty acids seem of particular interest since they are avidly taken up into the myocardium. In addition, areas of myocardial ischemia have been detected with radiolabeled fatty acids.^{20,21} Therefore, the bifunctional ligand *N*³,*N*⁶-bis-(2'-myristoyloxyethyl)-1,8-dioxotriethylenetetraamine-*N,N,N',N'*-tetraacetic acid (BME-DTTA, **1**; Scheme 1), which contains two myristoyl chains, was designed and synthesized in our laboratory.²²⁻²⁴ The fatty acyl moiety can anchor into the phospholipid bilayer resulting in long tissue retention time of the contrast agent. The metal-binding moiety (an amide-EDTA-like analogue) would protrude into the extracellular water space modifying local water proton relaxation rates. The complex Gd(BME-DTTA), however, has a low solubility in water, attributable to the presence of the two long

myristoyl chains. Therefore, the complex has been prepared in the presence of a lipophilic environment such as egg lecithin liposomes.²⁵

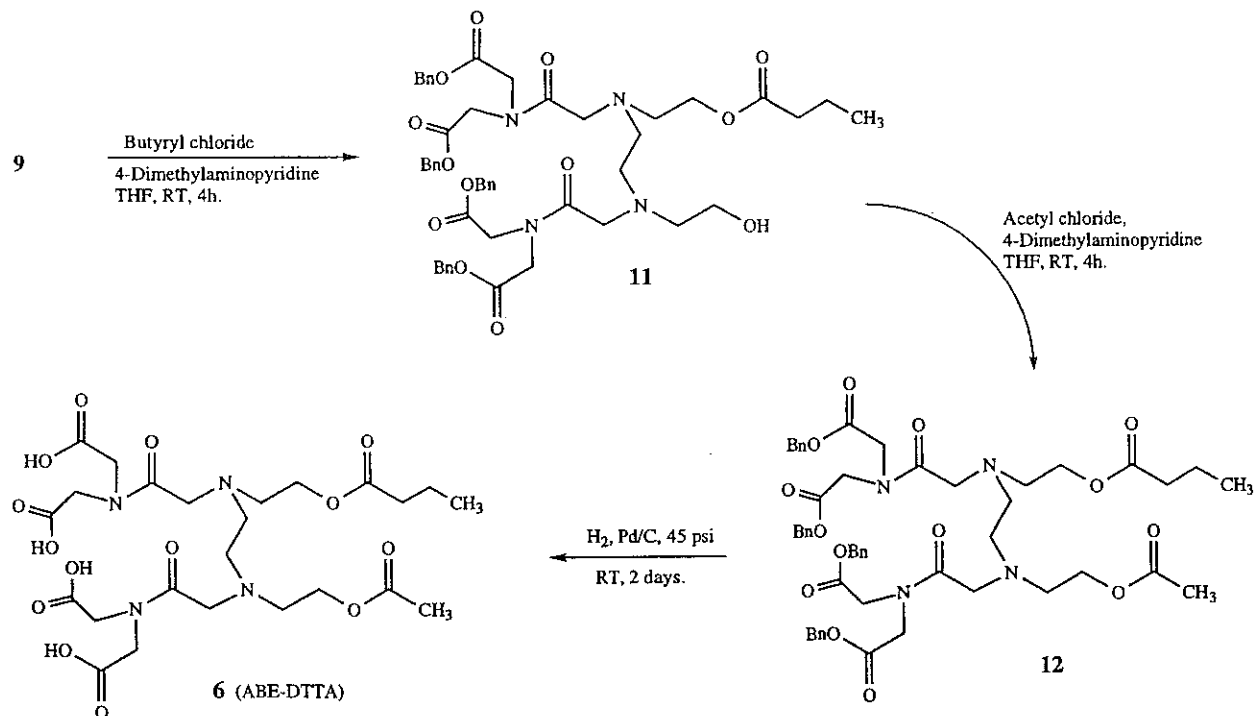
Our aim has been to develop a clinically applicable, lipophilic, metal-binding bifunctional cardiac-specific contrast agent that can be administered intravenously. Such agent should (1) be water soluble; (2) have the ability to complex with paramagnetic metal ions, in particular with gadolinium; (3) be nontoxic; (4) enable high proton relaxation rate enhancements; (5) be preferentially retained in the myocardium in proportion to perfusion; (6) have a relatively long lifetime in tissue and blood pool in combination with differential uptake between affected and normal tissue.

A logical approach to improve the solubility of the agent was to shorten the fatty acyl chain. Therefore, short chain analogues of BME-DTTA (Scheme 1) (BAE-DTTA (**2**), BPE-DTTA (**3**), BBE-DTTA (**4**), and BHE-DTTA (**5**)) were synthesized as ligands for the proposed cardiac-specific contrast agents. These analogues were symmetrically substituted derivatives where the two fatty acyl chains are identical. In addition, we also synthesized an asymmetric analogue, ABE-DTTA (**6**; Scheme 2), where the two fatty acyl chains are different. The solubility, relaxivity, and in vivo efficacy of the gadolinium complexes of these analogues were tested to evaluate their ability to induce specific MRI signal intensity enhancements in cardiac tissue.

Chemistry

Synthesis. The synthesis of the symmetric analogues **1-5** was achieved as depicted in Scheme 1. Intermedi-

Scheme 2



ate 7 was synthesized according to a previously published procedure.²² Addition of 7 to commercially available *N,N*-bis(2-hydroxyethyl)ethylenediamine (8) in the presence of triethylamine afforded intermediate 9. Treatment of 9 with myristoyl chloride, acetyl chloride, propionyl chloride, butyryl chloride, or hexanoyl chloride afforded bis-myristoyl 10a, bis-acetyl 10b, bis-propionyl 10c, bis-butyryl 10d, and bis-hexanoyl 10e analogues, respectively. Hydrogenolysis of intermediates 10 afforded the symmetric target compounds 1–5.

For the synthesis of monobutyrate compound 11 (Scheme 2), stoichiometric amounts of considerably pure 9 and butyryl chloride were used to reduce the probability of forming the symmetric bis-butyryl analogue. Purification of intermediate 9 via silica gel chromatography was not practical, resulting in a very low yield. Intermediate 9 was treated with 1 equiv of butyryl chloride in a dilute medium to give monobutyryl 11 (30–40% yield) and a mixture of bis-butyryl analogue and the starting material 9. Acetylation of 11 using acetyl chloride yielded 12 (78% yield), which after hydrogenolysis afforded the desired asymmetric analogue 6 with an 88% yield.

Relaxivity. The proton NMR longitudinal relaxation rate ($1/T_1$) of water in the presence of each (1:1) gadolinium–ligand complex was measured at pH 7.0 and 40 °C, on an IBM PC-20 (0.47 T) Minispec NMR instrument, using an inversion recovery sequence with eight delay times. For each sample, the final relaxation rate, R_1 , was calculated from the average of three consecutive $1/T_1$ measurements. The longitudinal relaxivity, $\rho_1 \pm \text{SEM}$ ($\text{s}^{-1} \text{mM}^{-1}$), for each complex was calculated and is reported in Table 1.

Relaxivity (ρ_1) is defined as the paramagnetic enhancement per unit concentration of the paramagnetic complex, i.e.,

$$\rho_1 = \Delta R_1 / c \quad (1)$$

Table 1. Specific Parameters of the Gadolinium Complexes of Substituted DTTA

complex	MW ^a	aqueous solubility (mM)	ρ_1 ($\text{s}^{-1} \text{mM}^{-1}$) 0.47 T	ρ_1 ($\text{s}^{-1} \text{mM}^{-1}$) ^b 0.47 T
Gd(BAE-DTTA)	578.55	30	14.05 ± 0.14	N/A
Gd(BPE-DTTA)	606.52	7	12.02 ± 0.08	21.57 ± 1.4
Gd(ABE-DTTA)	606.52	25	16.32 ± 0.32	N/A
Gd(BBE-DTTA)	634.62	5	13.91 ± 0.21	20.32 ± 0.5
Gd(BHE-DTTA)	690.73	0.5	15.65 ± 0.10	23.10 ± 0.2
Gd(BME-DTTA)	915.18	0.015	19.65 ± 0.15	27.10 ± 0.3

^a Molecular weight of the ligand. ^b Longitudinal relaxivity of the complex in liposomal formulation.

where c is the concentration of the paramagnetic complex in millimolar units. The relaxivity ρ_1 is characteristic of a given Gd–ligand complex. The paramagnetic enhancement, ΔR_1 , is calculated by subtracting the diamagnetic $1/T_1$ of pure water from the observed relaxation rate:

$$\Delta R_1 = R_1 - 1/T_{1(\text{water})} \quad (2)$$

where R_1 is the observed relaxation rate for each sample and $T_{1(\text{water})}$ is the constant T_1 of pure water (3.7 s).

Solubility. The water solubility of the contrast agents Gd(BME-DTTA), Gd(BHE-DTTA), Gd(BBE-DTTA), Gd(BPE-DTTA), and Gd(ABE-DTTA) was studied. The solubility of each complex was defined as the highest concentration attained before precipitation was observed. The method used was to prepare the (1:1) Gd–ligand (GdL) complex of each ligand at varying nominal Gd^{3+} concentrations within a concentration range around the anticipated concentration of precipitation. The samples were adjusted to pH 7.0 and filtered using a filter with a 0.1- μm pore size to remove all undissolved complex. Subsequently, a 10-mm NMR tube was filled with 4 mL of the filtered solution, and R_1 was determined. Using this procedure, the final concentration of

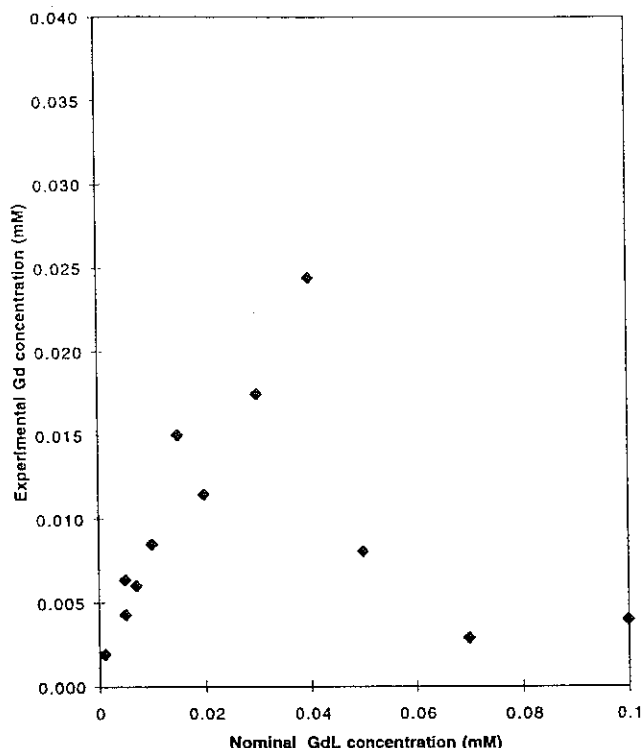


Figure 1. Experimental Gd concentration (mM) versus nominal GdL (mM) concentration of the least soluble system, Gd(BME-DTTA), in water at pH 7.

the filtrate was determined for each nominal concentration as follows: The concentration c can be determined by measuring gadolinium concentration using quantitative metal analyses for gadolinium content by inductively coupled plasma optical emission spectroscopy (ICP-OES) at Galbraith Laboratories. Once this is done for one well-dissolved concentration of each given complex, and ΔR_1 is also measured, the characteristic ρ_1 value is obtained for this complex from eq 1. This ρ_1 value is then used to calculate the experimental concentrations in all other samples of the same complex using the following formula:

$$c_{\text{experimental}} = \Delta R_{1(\text{observed})} / \rho_1 \quad (3)$$

This procedure is then repeated for all complexes.

The shape of a plot of the nominal concentration versus the experimental concentration of a Gd-ligand complex should reflect the solubility characteristics of this complex. An example, using the Gd(BME-DTTA) data, is shown in Figure 1. The highest complex concentration, where the experimental concentration is not yet significantly different from the corresponding nominal concentration, is defined as the solubility.

MRI. A 1.5 T Philips Gyroscan MRI imager with a head coil was used for ferret heart imaging. An ECG gated, relatively T_1 -weighted ($T_R = 600$ ms, $T_E = 30$ ms), spin-echo pulse sequence was set up in a multiple-slice, multiple-phase dynamic study. During the 10 min of each dynamic interval, nine images with three tomographic slices in three cardiac phases (two diastolic and one systolic phase) were obtained. Control images were obtained, and a bolus of 50 $\mu\text{mol/kg}$ Gd(BAE-DTTA), Gd(BPE-DTTA), Gd(ABE-DTTA), Gd(BBE-DTTA), or Gd(BHE-DTTA) was injected; MRI signal intensity en-

hancement was monitored over a 3-h interval. An agarose phantom in a plastic cup was used as an external intensity reference. Thus intensity enhancement is expressed by

$$\text{IE} = 100(I_{\text{post}} - I_{\text{pre}}) / I_{\text{pre}} \quad (4)$$

where $I_{\text{pre}} = I_{\text{heart}} / I_{\text{reference}}$ (before injection of the agent) and $I_{\text{post}} = I_{\text{heart}} / I_{\text{reference}}$ (after injection of the agent), with I denoting MRI signal intensity.²⁴

Results

Solubility. Figure 1 is a representative graph of the experimental Gd^{3+} concentration versus nominal GdL concentration which is used to determine the aqueous solubility of our contrast agents. In this figure we show data from the least soluble system, Gd(BME-DTTA). Below 0.015 mM nominal concentration, the solutions were clear and the experimentally determined concentrations were nearly equal to the nominal, suggesting the absence of precipitation. The samples between nominal concentrations of 0.015 and 0.04 mM were cloudy, indicating some precipitation, and indeed the experimental concentrations were significantly lower than the nominal concentrations. Obvious precipitation was observed above 0.04 mM, manifesting a dramatic limit of solubility, accompanied with a sharp deviation of the experimental concentrations from the nominal. On the basis of this graph, the solubility of the complex was determined as 0.015 mM.

Similar graphs for the gadolinium complexes of 2-5 in water at pH 7 revealed the following results: (1) For Gd(BHE-DTTA), a linear correlation was found between the nominal and experimental concentrations at a concentration below 0.5 mM and an abrupt reduction in the experimental concentration at a concentration of 1 mM and above. The solubility of the ligand was determined as 0.5 mM. (2) For Gd(BBE-DTTA), precipitation occurred slightly above 5 mM and sharply above 10 mM. The solubility of the agent was thus determined as 5 mM. (3) Similarly, the solubility of Gd(BPE-DTTA) was determined as 7 mM. Samples above 7 mM of Gd(BPE-DTTA) were cloudy. (4) For Gd(ABE-DTTA), a linear correlation was observed between experimental and nominal concentrations up to 25 mM. Clear precipitation was observed above 25 mM. The solubility of the agent was thus determined as 25 mM. (5) Gd(BAE-DTTA) is the most water soluble in this series, exhibiting a solubility of 30 mM.

In Figure 2, the solubilities of the entire series of complexes are plotted versus the number of fatty acyl carbon atoms in each complex. Thus, 4, 6, 8, 12, and 28 fatty acyl carbon atoms represent the complexes Gd(BAE-DTTA), Gd(ABE-DTTA) and Gd(BPE-DTTA), Gd(BBE-DTTA), Gd(BHE-DTTA), and Gd(BME-DTTA), respectively. The solubility decreases with the increase in the number of fatty acyl carbon atoms. The shortest symmetrically substituted agent, Gd(BAE-DTTA), has the highest water solubility (30 mM), followed by the asymmetrically substituted agent, Gd(ABE-DTTA) (25 mM). Therefore, an injectable sample of each of these two complexes can be prepared without the need for dispersing agents.

MRI. The ferrets were anesthetized, ventilated, and instrumented for iv line, blood pressure recording, and

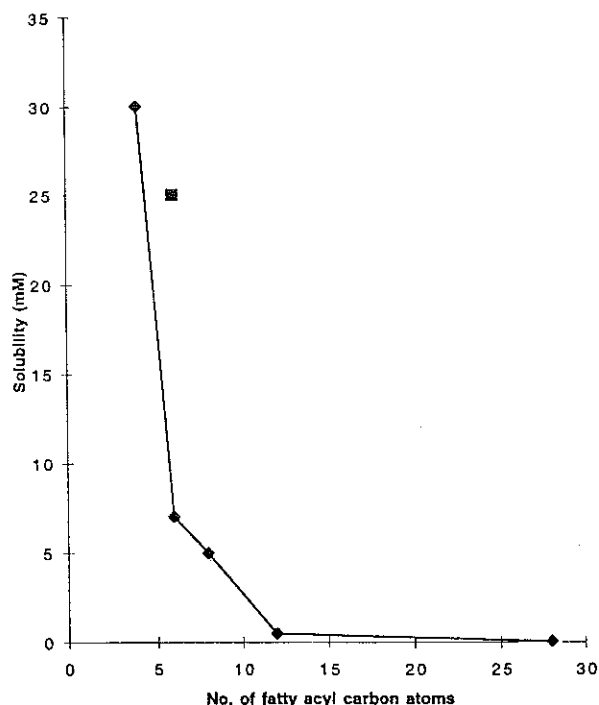


Figure 2. Dependence of contrast agent aqueous solubility on fatty acyl chain length. The solubility (mM) of each complex in the series versus the total number of fatty acyl carbon atoms in each complex is plotted. Thus, 4, 6, 8, 12, and 28 fatty acyl carbon atoms represent the symmetric complexes Gd(BAE-DTTA), Gd(BPE-DTTA), Gd(BBE-DTTA), Gd(BHE-DTTA), and Gd(BME-DTTA), respectively (filled diamonds, see ligand structures in Scheme 1); 6 fatty acyl carbon atoms represent also the asymmetric complex Gd(ABE-DTTA) (filled square, see ligand structure in Scheme 2).

Table 2. In Vivo Myocardial MRI IE in Ferrets Induced by (50 $\mu\text{mol/kg}$) Gadolinium Complexes of Substituted DTTA

complex	IE (%)		
	0–10 min	30–60 min	at 180 min
Gd(BAE-DTTA)	87.2 \pm 21	10.1 \pm 12	10.1 \pm 12
Gd(BPE-DTTA) ^a	34.6 \pm 8.9	38.4 \pm 8.7	47.2 \pm 8
Gd(ABE-DTTA)	42.8 \pm 5	43.6 \pm 4	38.5 \pm 3.5
Gd(BBE-DTTA) ^a	53.1 \pm 8.1	52.1 \pm 5.6	39.3 \pm 7
Gd(BHE-DTTA) ^a	32.3 \pm 6.3	41.7 \pm 7.1	30.1 \pm 5.7
Gd(BME-DTTA) ^a	55.2 \pm 9	67.2 \pm 12	65.2 \pm 9

^a The liposomal formulation of the complex was injected.

ECG. To examine the effect of our contrast agent on heart function, the heart rate and blood pressure was continuously monitored before and after any contrast agent injected. During our recent MRI experiments and in our previous studies,^{24,25} the heart rate of the ferrets remained within the 210–240 beats/min range, and systolic and diastolic pressures remained within the ranges of 210–225 and 160–170 mmHg, respectively.

In healthy ferrets, following the administration of 50 $\mu\text{mol/kg}$ liposomal Gd(BME-DTTA), the overall enhancement of the myocardial MRI signal intensity (MRI IE), induced by this agent, was studied. The signal intensity in heart muscle increased by 55.2 \pm 9% ($p < 0.001$) within 10 min after administration of agent. In subsequent images, obtained during the first hour after agent administration, a 67.2 \pm 12% MRI IE in the myocardium was observed (Table 2). Beyond the first hour, the average intensity remained at a plateau level for 3 h

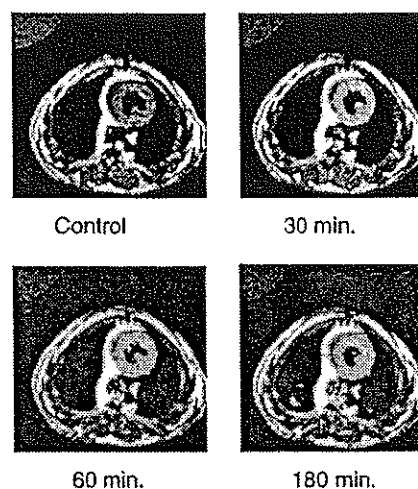


Figure 3. Gd(ABE-DTTA) (50 $\mu\text{mol/kg}$) enhanced proton MRI images of ferret heart obtained in vivo. A 1.5 T Philips Gyroscan with a head coil was used for ferret heart imaging. Representative images are shown for pre-agent control and at different times following agent administration. Note the clear brightening of the heart tissue in the post-agent images as compared to pre-agent control. An agarose phantom in a plastic cup seen in the upper left corner was used as an external intensity reference.

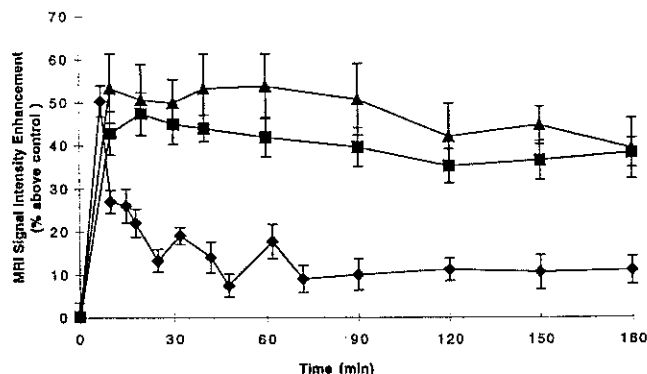


Figure 4. Time dependence of the Gd(ABE-DTTA) (filled squares), Gd(BAE-DTTA) (filled diamonds), and Gd(BBE-DTTA) (filled triangles) induced myocardial IEs obtained from the images of the type shown in Figure 3.

indicating a reasonably long lifetime of this contrast agent in heart tissue.²⁴

In similar experiments, injecting 50 $\mu\text{mol/kg}$ liposomal Gd(BPE-DTTA), Gd(BBE-DTTA) (Figure 4), or Gd(BHE-DTTA), a 34.6 \pm 8.9%, 53.1 \pm 8.1%, or 32.3 \pm 6.3% MRI IE in the myocardium was observed, respectively, within 10 min after agent administration (Table 2). All these agents showed lifetimes in the heart tissue similar to that of Gd(BME-DTTA).

The myocardial MRI IE, induced by 50 $\mu\text{mol/kg}$ of the water-soluble agent Gd(ABE-DTTA), is demonstrated in Figure 3. Representative images are shown for pre-agent control and at 30, 60, and 180 min following agent administration. Note the clear brightening of the heart tissue at these three time points as compared to control. The signal intensity in heart muscle increased by 42.8 \pm 5% ($p < 0.001$) within 15 min after agent administration. In subsequent images, obtained during the first hour, a 43.6 \pm 4% MRI IE in the myocardium was still observed. Beyond the first hour, the average intensity decreased only slightly and at a slow rate during 3 h,

indicating a reasonably long lifetime of the contrast agent in the heart tissue (Table 2, Figure 4).

Gd(BAE-DTTA), the symmetrically substituted water-soluble agent, at 50 $\mu\text{mol/kg}$ induced an MRI IE of $87.2 \pm 21\%$ within 2 min of administration. The MRI IE decreased to 50% after 5 min and gradually diminished (Table 2, Figure 4).

Discussion

The dominant effect of a paramagnetic agent in MRI is to increase the signal intensity of the tissue containing the agent.¹⁹ The extent of a contrast agent (CA)-induced MRI IE, using a T_1 -weighted acquisition sequence, primarily depends on the injected dose of the CA.

The distribution of the CA during myocardial ischemia should be proportional to the myocardial perfusion. Thus a concentration differential of the CA between ischemic and nonischemic regions is created. This differential generates regional differences in the T_1 values which can be visualized in T_1 -weighted MRI. Thus acute myocardial ischemic regions can be depicted as relatively dark regions by using CA-enhanced, T_1 -weighted MRI. Unfortunately, however, the dose of the CA cannot be increased above 0.2 mmol/kg, since T_2 shortens, and no further increase in MRI IE occurs in proportion with the additional increase in the dosage of the CA.¹⁹

A practical CA should induce a considerable MRI IE when administered at a dose of approximately 50 $\mu\text{mol/kg}$ weight of subject. In addition, the agent should be considerably water soluble allowing the formulation of this dose in a volume which is reasonable for injection. Gd(BME-DTTA) with its water solubility of 0.01 mM clearly would require too large a volume. By incorporating this complex in liposomes, the injectable volume becomes manageable. Liposomal formulations, however, suffer from disadvantages, including limited shelf life.

The gadolinium complexes of the long chain symmetrically substituted analogues (Scheme 1) BME-DTTA (1), BPE-DTTA (3), BBE-DTTA (4), and BHE-DTTA (5) tend to precipitate below the required concentration for injection (12–15 mM). Therefore, all these complexes had to be prepared in the presence of a lipophilic environment such as egg lecithin liposomes. These liposomal gadolinium complexes have the remarkably high relaxivities of 27.1, 21.57, 20.32, and 23.1 $\text{s}^{-1} \text{mM}^{-1}$, respectively (Table 1).

Compared to Gd(DTPA) ($\rho_1 = 4.1 \text{ s}^{-1} \text{mM}^{-1}$),²⁶ the liposomal Gd(BME-DTTA) complex has a 5 times higher relaxivity. Consequently, a 5 times lower dose of liposomal Gd(BME-DTTA) may be administered and still observe similar relaxation effects. Similarly, the water-soluble Gd(BAE-DTTA) and Gd(ABE-DTTA) complexes have 3 times higher relaxivities (14.05 and 16.32 $\text{s}^{-1} \text{mM}^{-1}$, respectively), enabling the reduction of their effective doses by a factor of 3.

Following the injection of 50 $\mu\text{mol/kg}$ body weight of the liposomal gadolinium complexes of 1, 3, 4, or 5 to live ferrets, a sustained enhancement in MRI signal intensity in the myocardium ($67.2 \pm 12\%$, $38.4 \pm 8.7\%$, $52.1 \pm 5.6\%$, $41.7 \pm 7.1\%$, respectively) is induced without deleterious effects on heart function parameters. However, this liposomal formulation is less than

favorable due to the heterogeneity of the particle sizes in the suspension resulting in a different uptake by the different organs (spleen, kidney, liver). Electron micrographs of liposomal Gd(BME-DTTA) suspension revealed an average particle size smaller than 0.125 μm and a mixture of vesicular and discoidal structures. The formation of a discoidal structure could be explained by the tendency of the long myristoyl chains of the BME-DTTA ligand to associate with the outer surface of the disk formed by the phosphatidylcholine.²⁵ The surfactant molecule, cholesterol, was used during the preparation of liposomal Gd(BME-DTTA) to prevent the fusion of small sonicated liposomes.²⁷ Such fusion, if occurred, would decrease the surface-to-volume ratio of the vesicles resulting in a reduction in relaxivity. In addition, the sample had to be stored at 4 °C to retain its relaxivity. With time, deterioration in liposome chemistry might occur at room temperature, resulting in a dramatic decrease of relaxivity. Consequently, these complexes cannot be considered as practical contrast agents.

The gadolinium complex of 2, with its symmetric short chain substitution, was water soluble at the concentration range required for injection. Although the agent induced a remarkable MRI IE, it exhibited a relatively short half-life in tissue. Thus this agent displayed a Magnevist-like kinetics indicating a loss of the typical behavior of our agent line exemplified by that of Gd(BME-DTTA). The fatty acyl asymmetrically substituted analogue 6 proved its potential use as a water-soluble, cardiac-specific CA. The complex Gd(ABE-DTTA) is completely soluble in water at 25 mM concentration allowing the preparation of a reasonable volume for bolus injection to achieve a 50 $\mu\text{mol/kg}$ dose. The presence of the acetyl group improves the solubility of Gd(ABE-DTTA) compared to Gd(BPE-DTTA), although these two complexes contain the same total number of fatty acyl carbon atoms. The measured relaxivity of this complex was 16.24 $\text{s}^{-1} \text{mM}^{-1}$. The agent showed a specific accumulation in canine heart tissue within 15 min after administration, inducing a sustained MRI IE of $43.6 \pm 4\%$. This enhancement lasted for at least 3 h, including a period of 30 min of ischemia and 40 min of reperfusion, indicating a reasonably long lifetime of this CA in the myocardium.

The LD_{50} for Gd^{3+} aqua ion is 0.5 mmol/kg following iv administration to rats.²⁸ GdCl_3 , however, cannot be injected intravenously due to its insolubility at physiological pH and to its high affinity for the calcium-binding sites of a living being, owing to its greater charge/radius ratio.¹⁰ An LD_{50} of 0.56 mmol/kg for liposomal Gd(BME-DTTA) has been published.²⁵ The LD_{50} values for the Gd complexes of other BME analogue complexes were in the same range, i.e., ~ 0.6 mmol/kg, as we expected, based on the relative similarity of their stability constants.^{22,23} The LD_{50} of the ligands should be similar to this ~ 0.6 mmol/kg range. The effective MRI dose is less than one-tenth of this LD_{50} . Thus, it can be used safely in vivo.

The myocardial specificity of liposomal Gd(BME-DTTA) was already observed in our previous ferret experiments.^{24,25} It is our experience that the gadolinium complexes of BME-DTTA and its analogues induce the highest IE in the heart among all organs. It is our hypothesis that this myocardial specificity results

from the fatty acid chain of our compounds. The critical length of the fatty acid chain for specific, sustained myocardial signal IE is probably due to the presence of at least one butyryl chain in the chelator ligand as we show in this study. We do not expect differences in the IE-inducing process between liposomal and non-liposomal preparations, once the compounds are already at the target organ. We expect, however, differences as the compounds are carried to the target, i.e., either with small liposome particles or with the help of plasma proteins.

Conclusions

Our goal was the synthesis of BME-DTTA-like ligands whose gadolinium complexes would exhibit improved water solubility. The gadolinium complexes of analogues 1 and 3–5 tended to precipitate at very low concentration and thus had to be prepared in liposomal milieu. Although high relaxivity was preserved in the liposomal systems, and sustained myocardial MRI IE was induced, these liposomal preparations had practical disadvantages. On the other hand, while the symmetrically substituted short chain complex Gd(BAE-DTTA) was very water soluble, it showed a very short lifetime in the blood stream and in tissue, and thus its IE disappeared after 15 min following injection. Consequently, this complex could not be considered as a practical contrast agent. The asymmetrically substituted Gd-(ABE-DTTA), however, retained a long-lived, specific myocardial MRI IE.

Our preliminary *in vivo* studies with Gd(ABE-DTTA) have proven that this agent could be useful for MRI diagnosis of ischemic heart disease. The agent (1) is water soluble at 10 mM concentration suitable enough to be injected in an *in vivo* experiment; (2) displays a relaxivity 3 times higher than that of the widely used contrast agent, Gd(DTPA); (3) shows a specific accumulation in the myocardial tissue; and (4) induces a sustained MRI signal intensity enhancement lasting 180 min.

Experimental Section

All reagents (above 97% purity) were purchased from Aldrich Chemical Co. and Sigma Co. (Milwaukee, WI) and were used without further purification. Preparative scale chromatography was carried out using E. Merck silica gel 60, 230–440 mesh. Thin-layer chromatography was conducted on Merck precoated silica gel 60 F-254. All ^1H NMR spectra were recorded on a Bruker AM-360 NMR spectrometer, and all chemical shifts are reported as δ (ppm) values referenced to TMS. Infrared spectra were recorded on a Perkin-Elmer 1600 series FT-IR spectrophotometer. All electrospray ionization mass spectrometry experiments were performed on a PE-Sciex (Concord, Ontario, Canada) API-III triple-quadrupole mass spectrometer equipped with an atmospheric pressure ion source. In all cases, ^1H NMR, MS, and IR spectra were consistent with assigned structures. Elemental microanalyses were performed by Atlantic Microlab Inc., Norcross, GA, or by Galbraith Laboratories, Knoxville, TN, and were within $\pm 0.4\%$ of calculated values.

N,N-Bis(benzoyloxycarbonylmethyl)bromoacetamide (7) was synthesized from dibenzyl iminodiacetate according to a previously published procedure.²²

N,N-Bis(2-hydroxyethyl)-*N,N*-bis[*N,N'*-bis(benzoyloxycarbonylmethyl)acetamido]-1,2-ethanediamine (9). A suspension of *N,N*-bis(2-hydroxyethyl)ethylenediamine (8) (10.875 g, 0.07338 mol) and triethylamine (15.15 g, 0.1497 mol), in 60

mL of dry DMF under nitrogen atmosphere at 0 °C, was treated with a solution of compound 7 (65 g, 0.149 mol) in 70 mL of dry DMF. The reaction was stirred at 0 °C for 1 day. The precipitate was filtered, and the filtrate was concentrated under reduced pressure to give the crude product as a brown oil. The crude product was then treated with water and chloroform. The chloroform layer was separated, washed with water, dried over MgSO_4 , and concentrated to give a clean product 9 (57 g, 90%) which was used for the next step without further purification. Purification by silica gel column chromatography was found to be impractical resulting in a very low yield. ^1H NMR in CDCl_3 (ppm): 2.62 (s–t, 4H, N $\text{CH}_2\text{CH}_2\text{N}$), 2.68 (s–t, 4H, 2 $\text{OHCH}_2\text{CH}_2\text{N}$), 3.4 (s, 4H, 2 NCH_2CON), 3.5 (m, 4H, 2 $\text{HOCH}_2\text{CH}_2\text{N}$), 4.17, 4.26 (2s, 8H, 4 NCH_2COO), 5.09, 5.15 (2s, 8H, 4 CH_2 benzylic), 7.33 (s, 20H, aromatic). $\text{C}_{46}\text{H}_{54}\text{N}_4\text{O}_{12}$, MS (m/z): 855 (MH^+).

N,N'-Bis(2-acetyloxyethyl)-*N,N'*-bis[*N,N'*-bis(benzoyloxycarbonylmethyl)acetamido]-1,2-ethanediamine (10b). A 3.86-g portion (0.0245 mol) of compound 9 was dissolved in 330 mL of dry THF under nitrogen atmosphere. Acetyl chloride (0.7 g, 0.009 mol) was added dropwise. 4-(Dimethylamino)pyridine (1.1 g, 0.009 mol) was added, and the reaction was allowed to stir at room temperature for 4 h and then filtered. Water and chloroform were added. The chloroform layer was separated, extracted with saturated NaHCO_3 and saturated NaCl, dried over MgSO_4 , filtered, and removed by rotavapor. Purification was accomplished using silica gel column chromatography and elution with hexane:EtOAc (3:7) yielding the bis-acetyl analogue 10b (2.1 g, 50%) as a yellow oil. ^1H NMR in CDCl_3 (ppm): 1.98 (s, 6H, 2 CH_3COO), 2.62 (m, 4H, $\text{NCH}_2\text{CH}_2\text{N}$), 2.73 (t, 4H, 2 $\text{OCOCH}_2\text{CH}_2\text{N}$), 3.41 (s, 4H, 2 NCH_2CON), 4.07 (t, 4H, 2 $\text{OCOCH}_2\text{CH}_2\text{N}$), 4.17, 4.43 (2s, 8H, 4 NCH_2COO), 5.12, 5.15 (2s, 8H, 4 CH_2 benzylic), 7.33 (s, 20H, aromatic). IR (cm^{-1}) (on NaCl plates): 2959, 1739, 1660, 1457, 1379, 1240, 1179, 1041, 984, 741, 699. $\text{C}_{50}\text{H}_{58}\text{N}_4\text{O}_{14}$, MS (m/z): 940 (MH^+).

N,N'-Bis(2-acetyloxyethyl)-*N,N'*-bis[*N,N'*-bis(carboxymethyl)acetamido]-1,2-ethanediamine (BAE-DTTA, 2). A 2.88-g portion (0.0030 mol) of compound 10b was dissolved in 40 mL of ethanol. Pd/C (0.35 g, 15% w/w) was wetted with ethanol and added. The suspension was hydrogenated at 40 psi in a Parr apparatus at room temperature for 2 days. The catalyst was filtered off (0.45- μm Zetapore filter), dried, and recrystallized from ethanol/chloroform to give 1.3 g (75%) of the crude product 2 as white crystals. ^1H NMR in D_2O (ppm): 2.14 (s, 6H, 2 CH_3COOCO), 3.29 (m, 4H, $\text{NCH}_2\text{CH}_2\text{N}$), 3.39 (m, 4H, 2 $\text{OCOCH}_2\text{CH}_2\text{N}$), 4.08, 4.10 (2s, 4H, 2 NCH_2CON), 4.22, 4.28 (2s, 8H, 4 NCH_2COO), 4.34 (t, 4H, 2 $\text{OCOCH}_2\text{CH}_2\text{N}$). IR (cm^{-1}) (KBr) 3434 (vb), 2964 (vb), 2583 (vb), 1735, 1659, 1463, 1381, 1234, 1180, 1049, 973, 880, 842, 755, 640, 597. MS (m/z): 579 (MH^+). Anal. ($\text{C}_{22}\text{H}_{34}\text{N}_4\text{O}_{14}$) C, H, N.

N,N'-Bis(2-propionyloxyethyl)-*N,N'*-bis[*N,N'*-bis(benzoyloxycarbonylmethyl)acetamido]-1,2-ethanediamine (10c). A 3.4-g portion (0.00397 mol) of compound 9 was dissolved in 20 mL of dry THF under nitrogen atmosphere and treated with propionyl chloride (0.7369 g, 0.0079 mol) and 4-(dimethylamino)pyridine (0.97 g, 0.0079 mol) as described for 10b. Purification was accomplished using silica gel column chromatography and elution with hexane:EtOAc (1:1) yielding the bis-propionyl analogue 10c (1.9 g, 49%) as a yellow oil. ^1H NMR in CDCl_3 (ppm): 1.98 (s, 6H, 2 CH_3COO), 2.62 (m, 4H, $\text{NCH}_2\text{CH}_2\text{N}$), 2.73 (t, 4H, 2 $\text{OCOCH}_2\text{CH}_2\text{N}$), 3.41 (s, 4H, 2 NCH_2CON), 4.07 (t, 4H, 2 $\text{OCOCH}_2\text{CH}_2\text{N}$), 4.17, 4.43 (2s, 4H, 2 NCH_2COO), 5.12, 5.15 (2s, 8H, 4 CH_2 benzylic), 7.33 (s, 20H, aromatic). IR (cm^{-1}) (on NaCl plates): 2947, 2844, 1741, 1661, 1457, 1383, 1354, 1240, 1180, 1081, 988, 742, 699. $\text{C}_{52}\text{H}_{62}\text{N}_4\text{O}_{14}$, MS (m/z): 968 (MH^+).

N,N'-Bis(2-propionyloxyethyl)-*N,N'*-bis[*N,N'*-bis(carboxymethyl)acetamido]-1,2-ethanediamine (BPE-DTTA, 3). A 1.87-g portion (0.0019 mol) of compound 10c was dissolved in 20 mL of ethanol. Pd/C (0.27 g, 15% w/w) was

added, and the suspension was hydrogenated as described for **10b**, dried, and recrystallized from ethanol/chloroform to give 0.45 g (38%) of the crude product **3** as white crystals. $^1\text{H NMR}$ in D_2O (ppm): 1.54 (t, 6H, 2 $\text{CH}_3\text{CH}_2\text{COO}$), 2.42 (q, 4H, 2 $\text{CH}_3\text{CH}_2\text{COO}$), 3.28 (m, 4H, $\text{NCH}_2\text{CH}_2\text{N}$), 3.38 (m, 4H, 2 $\text{OCOCH}_2\text{CH}_2\text{N}$), 4.06 (2s, 4H, 2 NCH_2CON), 4.18 (2s, 8H, 4 NCH_2COO), 4.36 (t, 4H, 2 $\text{OCOCH}_2\text{CH}_2\text{N}$). IR (cm^{-1}) (KBr): 3434 (vb), 2964 (vb), 2583 (vb), 1735, 1659, 1463, 1381, 1234, 1180, 1049, 973, 880, 842, 755, 640, 597. MS (m/z): 607 (MH^+). Anal. ($\text{C}_{24}\text{H}_{38}\text{N}_4\text{O}_{14} \cdot 0.5\text{H}_2\text{O}$) C, H, N.

***N,N'*-Bis(2-butyryloxyethyl)-*N,N'*-bis[*N,N'*-bis(benzyl-oxycarbonylmethyl)acetamido]-1,2-ethanediamine (10d)**. A 2.1-g portion (0.0024 mol) of compound **9** was dissolved in 30 mL of dry THF under nitrogen atmosphere and treated with butyryl chloride (0.523 mL) and 4-(dimethylamino)pyridine (0.6 g, 0.0049 mol) as explained for **10b**. Purification was accomplished using silica gel column chromatography and elution with hexane:EtOAc (1:1) yielding the bis-butyryl analogue **10d** (1.19 g, 50%) as a yellow oil. $^1\text{H NMR}$ in CDCl_3 (ppm): 0.91 (t, 6H, 2 $\text{CH}_3\text{CH}_2\text{CH}_2\text{COO}$), 1.61 (q, 4H, 2 $\text{CH}_3\text{CH}_2\text{CH}_2\text{COO}$), 2.23 (t, 4H, 2 $\text{CH}_3\text{CH}_2\text{CH}_2\text{COO}$), 2.62 (m, 4H, $\text{NCH}_2\text{CH}_2\text{N}$), 2.73 (t, 4H, 2 $\text{OCOCH}_2\text{CH}_2\text{N}$), 3.41 (s, 4H, 2 NCH_2CON), 4.07 (t, 4H, 2 $\text{OCOCH}_2\text{CH}_2\text{N}$), 4.04, 4.43 (2s, 4H, 2 NCH_2COO), 5.12 (2s, 8H, 4 CH_2 benzylic), 7.33 (s, 20H, aromatic). IR (cm^{-1}) (on NaCl plates): 2963, 2959, 2877, 1741, 1661, 1457, 1383, 1301, 1248, 1179, 991, 742, 699. $\text{C}_{57}\text{H}_{86}\text{N}_4\text{O}_{14}$, MS (m/z): 996 (MH^+).

***N,N'*-Bis(2-butyryloxyethyl)-*N,N'*-bis[*N,N'*-bis(carboxymethyl)acetamido]-1,2-ethanediamine (BBE-DTTA, 4)**. A 0.7-g portion (0.0007 mol) of compound **10d** was dissolved in 15 mL of ethanol. Pd/C (0.19 g, 15% w/w) was added, and the suspension was hydrogenated as described for **10b**, dried, and recrystallized from ethanol/chloroform to give 0.24 g (53%) of the crude product **4** as white crystals. $^1\text{H NMR}$ in D_2O (ppm): 0.88 (t, 6H, 2 $\text{CH}_3\text{CH}_2\text{CH}_2\text{COO}$), 1.62 (q, 4H, 2 $\text{CH}_3\text{CH}_2\text{CH}_2\text{COO}$), 2.41 (t, 4H, 2 $\text{CH}_3\text{CH}_2\text{CH}_2\text{COO}$), 3.34 (m, 4H, $\text{NCH}_2\text{CH}_2\text{N}$), 3.42 (m, 4H, 2 $\text{OCOCH}_2\text{CH}_2\text{N}$), 4.13, 4.15 (2s, 4H, 2 NCH_2CON), 4.24, 4.28 (2s, 8H, 4 NCH_2COO), 4.36 (t, 4H, 2 $\text{OCOCH}_2\text{CH}_2\text{N}$). IR (cm^{-1}) (KBr): 3434 (vb), 2964 (vb), 2583 (vb), 1735, 1659, 1463, 1381, 1234, 1180, 1049, 973, 880, 842, 755, 640, 597. MS (m/z): 635 (MH^+). Anal. ($\text{C}_{26}\text{H}_{42}\text{N}_4\text{O}_{14} \cdot 1.9\text{H}_2\text{O}$) C, H, N.

***N,N'*-Bis(2-hexanoyloxyethyl)-*N,N'*-bis[*N,N'*-bis(benzyl-oxycarbonylmethyl)acetamido]-1,2-ethanediamine (10e)**. A 3.04-g portion (0.00355 mol) of compound **9** was dissolved in 15 mL of dry THF under nitrogen atmosphere and treated with hexanoyl chloride (1.052 g, 0.007117 mol) and 4-(dimethylamino)pyridine (2.199 g, 0.018 mol) as explained for **10b**. Purification was accomplished using silica gel column chromatography and elution with hexane:EtOAc (1:1) yielding the bis-hexanoyl analogue **10e** (1.6 g, 42%) as a yellow oil. $^1\text{H NMR}$ in CDCl_3 (ppm): 0.91 (t, 6H, 2 $\text{CH}_3\text{CH}_2\text{CH}_2\text{CH}_2\text{CH}_2\text{COO}$), 1.61 (q, 12H, 2 $\text{CH}_3\text{CH}_2\text{CH}_2\text{CH}_2\text{CH}_2\text{COO}$), 2.23 (t, 4H, 2 $\text{CH}_3\text{CH}_2\text{CH}_2\text{CH}_2\text{CH}_2\text{COO}$), 2.62 (m, 4H, $\text{NCH}_2\text{CH}_2\text{N}$), 2.73 (t, 4H, 2 $\text{OCOCH}_2\text{CH}_2\text{N}$), 3.41 (s, 4H, 2 NCH_2CON), 4.07 (t, 4H, 2 $\text{OCOCH}_2\text{CH}_2\text{N}$), 4.04, 4.43 (2s, 8H, 4 NCH_2COO), 5.12, 5.15 (2s, 8H, 4 CH_2 benzylic), 7.33 (s, 20H, aromatic). IR (cm^{-1}) (on NaCl plates): 2959, 2864, 1741, 1661, 1457, 1383, 1240, 1180, 986, 742, 698. $\text{C}_{58}\text{H}_{74}\text{N}_4\text{O}_{14}$, MS (m/z): 1052 (MH^+).

***N,N'*-Bis(2-hexanoyloxyethyl)-*N,N'*-bis[*N,N'*-bis(carboxymethyl)acetamido]-1,2-ethanediamine (BBE-DTTA, 5)**. A 1.6-g portion (0.00152 mol) of compound **10e** was dissolved in 15 mL of ethanol. Pd/C (0.19 g, 15% w/w) was added, and the suspension was hydrogenated as described for **10b**, dried, and recrystallized from ethanol/chloroform to give 0.76 g (72%) of the crude product **5** as white crystals. $^1\text{H NMR}$ in D_2O (ppm): 0.93 (t, 6H, 2 $\text{CH}_3\text{CH}_2\text{CH}_2\text{CH}_2\text{CH}_2\text{COO}$), 1.31 (q, 12H, 2 $\text{CH}_3\text{CH}_2\text{CH}_2\text{CH}_2\text{CH}_2\text{COO}$), 2.41 (t, 4H, 2 $\text{CH}_3\text{CH}_2\text{CH}_2\text{CH}_2\text{CH}_2\text{COO}$), 3.34 (m, 4H, $\text{NCH}_2\text{CH}_2\text{N}$), 3.42 (m, 4H, 2 $\text{OCOCH}_2\text{CH}_2\text{N}$), 4.13, 4.15 (2s, 4H, 2 NCH_2CON), 4.35 (2s, 8H, 4 NCH_2COO), 4.36 (t, 4H, 2 $\text{OCOCH}_2\text{CH}_2\text{N}$). IR (cm^{-1}) (KBr): 3434 (vb), 2964 (vb), 2583 (vb), 1735, 1659, 1463, 1381, 1234, 1180, 1049, 973, 880, 842, 755, 640, 597. MS (m/z): 690 (MH^+). Anal. ($\text{C}_{30}\text{H}_{50}\text{N}_4\text{O}_{14} \cdot 1\text{H}_2\text{O}$) C, H, N.

***N*-(2-Butyryloxyethyl)-*N'*-(2-hydroxyethyl)-*N,N*-bis[*N,N'*-bis(benzyl-oxycarbonylmethyl)acetamido]-1,2-ethanediamine (11)**. A 15.412-g portion (0.018 mol) of compound **9** was dissolved in 330 mL of dry THF under nitrogen atmosphere. Butyryl chloride (1.726 g, 0.0162 mol) was added dropwise, and the reaction mixture was stirred at room temperature overnight. 4-(Dimethylamino)pyridine (2.199 g, 0.018 mol) was added, the reaction mixture was stirred at room temperature for 1 h and filtered, and solvent was removed on a rotavapor to give the crude product as a mixture of the starting material, the bis-butyryl, and the desired monobutyryl analogues. Purification was accomplished using silica gel column chromatography and elution with hexane:EtOAc (3:7). The bis-butyryl analogue was eluted first, followed by a pure fraction of the desired monobutyryl analogue **11** as a yellow oil. The column was subsequently washed with CHCl_3 :MeOH: NH_4OH (900:50:3) to elute the rest of the product mixed with some of the starting material. This last fraction was subjected to a second step of chromatography using silica gel CHCl_3 :MeOH: NH_4OH (900:50:3) which gave a second, colored, pure fraction of the desired monobutyryl analogue **11** as a light-orange oil. The total collected amount of compound **11** was 5.548 g (37%). $^1\text{H NMR}$ in CDCl_3 (ppm): 0.91 (t, 3H, $\text{CH}_3\text{CH}_2\text{CH}_2\text{COO}$), 1.59 (q, 2H, $\text{CH}_3\text{CH}_2\text{CH}_2\text{COO}$), 2.24 (t, 2H, $\text{CH}_3\text{CH}_2\text{CH}_2\text{COO}$), 2.62 (m, 4H, $\text{NCH}_2\text{CH}_2\text{N}$), 2.66 (t, 2H, $\text{HOCH}_2\text{CH}_2\text{N}$), 2.76 (t, 2H, $\text{OCOCH}_2\text{CH}_2\text{N}$), 3.39, 3.45 (2s, 4H, 2 NCH_2CON), 3.48 (t, 2H, $\text{HOCH}_2\text{CH}_2\text{N}$), 4.07 (t, 2H, $\text{OCOCH}_2\text{CH}_2\text{N}$), 4.16, 4.38 (2d, 8H, 4 NCH_2COO), 5.11, 5.16 (2d, 8H, 4 CH_2 benzylic), 7.33 (s, 20H, aromatic). IR (cm^{-1}) (on NaCl plates): 3462, 2957, 1742, 1660, 1458, 1386, 1355, 1301, 1182, 1080, 986, 825, 741, 698. $\text{C}_{50}\text{H}_{60}\text{N}_4\text{O}_{13}$, MS (m/z): 925 (MH^+). Note: The following additional peak splittings [3.39, 3.45 (2s, 4H, 2 NCH_2CON), 4.16–4.18 (d, 4H, 2 NCH_2COO), 4.35–4.38 (d, 4H, 2 NCH_2COO), 5.110, 5.115 (d, 2H, CH_2 benzylic), 5.16 (d, 2H, CH_2 benzylic)] do not exist in the dihydroxy intermediate (**9**). These remarkable splittings are due, most likely, to a slowed rotation around the N–R bond induced by the acyl substitutions. This slow rotation causes the two methylene protons in all methylene groups to become magnetically nonequivalent.

***N*-(2-Butyryloxyethyl)-*N'*-(2-ethoxyethyl)-*N,N*-bis[*N,N'*-bis(benzyl-oxycarbonylmethyl)acetamido]-1,2-ethanediamine (12)**. A 5.548-g portion (0.006 mol) of compound **11** was dissolved in 50 mL of dry THF under nitrogen atmosphere. Acetyl chloride (0.8 g, 0.0101 mol) and 4-(dimethylamino)pyridine (0.879 g, 0.00719 mol) were added dropwise, the reaction mixture was stirred at room temperature for 5 h and filtered, and the solvent was removed on a rotavapor to give the crude product **12** as a dark-yellow oil. Purification was accomplished using silica gel column chromatography and elution with CHCl_3 :MeOH: NH_4OH (900:50:3) to give pure **12** (4.92 g, 85%) as a bright-yellow oil. $^1\text{H NMR}$ in CDCl_3 (ppm): 0.91 (t, 3H, 2 $\text{CH}_3\text{CH}_2\text{CH}_2\text{COO}$), 1.61 (q, 2H, $\text{CH}_3\text{CH}_2\text{CH}_2\text{COO}$), 1.98 (s, 3H, CH_3COO), 2.23 (t, 2H, $\text{CH}_3\text{CH}_2\text{CH}_2\text{COO}$), 2.62 (m, 4H, $\text{NCH}_2\text{CH}_2\text{N}$), 2.73 (t, 4H, 2 $\text{OCOCH}_2\text{CH}_2\text{N}$), 3.41 (s, 4H, 2 NCH_2CON), 4.07 (t, 4H, 2 $\text{OCOCH}_2\text{CH}_2\text{N}$), 4.04, 4.43 (2s, 8H, 4 NCH_2COO), 5.12, 5.15 (2s, 8H, 4 CH_2 benzylic), 7.33 (s, 20H, aromatic). IR (cm^{-1}) (on NaCl plates): 2959, 1741, 1661, 1457, 1383, 1240, 1180, 988, 737, 699. $\text{C}_{52}\text{H}_{62}\text{N}_4\text{O}_{14}$, MS (m/z): 968 (MH^+).

***N*-(2-Butyryloxyethyl)-*N'*-(2-ethoxyethyl)-*N,N'*-bis[*N,N'*-bis(carboxymethyl)acetamido]-1,2-ethanediamine (ABE-DTTA, 6)**. A 1.85-g portion (0.00191 mol) of compound **12** was dissolved in 20 mL of methanol. Pd/C (0.277 g, 15% w/w) was added, and the suspension was hydrogenated as described for **10b**, dried, and recrystallized from ethanol/chloroform to yield 0.87 g (75%) of pure product as white crystals. $^1\text{H NMR}$ in D_2O (ppm): 0.93 (t, 3H, $\text{CH}_3\text{CH}_2\text{CH}_2\text{COO}$), 1.62 (q, 2H, $\text{CH}_3\text{CH}_2\text{CH}_2\text{COO}$), 2.14 (s, 3H, CH_3COO), 2.41 (t, 2H, $\text{CH}_3\text{CH}_2\text{CH}_2\text{COO}$), 3.34 (m, 4H, $\text{NCH}_2\text{CH}_2\text{N}$), 3.42 (m, 4H, 2 $\text{OCOCH}_2\text{CH}_2\text{N}$), 4.13, 4.15 (2s, 4H, 2 NCH_2CON), 4.24, 4.28 (2s, 8H, 4 NCH_2COO), 4.36 (t, 4H, 2 $\text{OCOCH}_2\text{CH}_2\text{N}$). IR (cm^{-1}) (KBr): 3434 (vb), 2964 (vb), 2583 (vb), 1735, 1659,

1463, 1381, 1234, 1180, 1049, 973, 880, 842, 755, 640, 597. MS (*m/z*): 607 (MH⁺). Anal. (C₂₄H₃₈N₄O₁₄·2.5H₂O) C, H, N.

Solubility. Gd(BME-DTTA): This analogue carries two myristoyl chains which are the longest fatty acyl chains in our series of ligands. A 0.1 mM solution was prepared by suspending solid BME-DTTA (0.00915 g, 0.01 mmol) in 100 mL of water. The pH of this suspension was repeatedly adjusted to 7.0 with sodium hydroxide until all the suspended material was completely dissolved. A solution of 0.01 M GdCl₃ was prepared. A series of 5-mL samples with varying BME-DTTA concentrations (0.005, 0.007, 0.010, 0.020, 0.030, 0.040, 0.050, 0.070, 0.100 mM) was prepared by an appropriate dilution of a 0.1 mM stock solution, and GdCl₃ was added to achieve a 1:1 molar ratio of Gd(BME-DTTA).

Gd(BHE-DTTA): A 10 mM solution was prepared by suspending BHE-DTTA (0.069 g, 0.1 mmol) in 10 mL of water. The pH was repeatedly adjusted to 7.0 until all the material was completely dissolved. Samples with 0.005, 0.010, 0.020, 0.050, 0.100, 0.250, 0.500, 1.000, 3.000 mM Gd(BHE-DTTA) (1:1) were prepared.

Gd(BBE-DTTA): A 20 mM solution was prepared by dissolving BBE-DTTA (0.126 g, 0.2 mmol) in 10 mL of water at pH 7.0. Samples of 0.010, 0.050, 1.00, 3.00, 5.00, 7.00, 10.00 mM Gd(BBE-DTTA) (1:1) were prepared.

Gd(BPE-DTTA): A 25 mM solution was prepared by dissolving BPE-DTTA (0.121 g, 0.2 mmol) in 8 mL of water at pH 7.0. Samples of 0.50, 1.00, 5.00, 7.00, 10.00, 15.00 mM Gd(BPE-DTTA) (1:1) were prepared.

Gd(ABE-DTTA): A 40 mM solution was prepared by dissolving ABE-DTTA (0.242 g, 0.4 mmol) in 10 mL of water at pH 7.0. Samples of 1.00, 5.00, 10.00, 20.00, 25.00, 40.00 mM Gd(ABE-DTTA) (1:1) were prepared.

Gd(BAE-DTTA): A 50 mM solution was prepared by dissolving (0.290 g, 0.5 mmol) BAE-DTTA in 10 mL of water, and the pH of the clear solution was adjusted to 7.0. Samples of 1.00, 5.00, 10.00, 20.00, 12.00, 15.00, 25.00, 40.00, 50.00 mM Gd(BAE-DTTA) (1:1) were prepared.

Solubility of each of the above complexes was determined as shown for Gd(BME-DTTA) in Figure 1. The solubility values obtained were then plotted in Figure 2 versus the number of fatty acyl carbon atoms to demonstrate the dependence of the aqueous solubility of these contrast agents on their total fatty acyl chain length.

Preparation of Injectable Formulations. Liposomal Gd(BPE-DTTA), Gd(BBE-DTTA), Gd(BHE-DTTA), and Gd(BME-DTTA): The gadolinium complexes of these ligands were incorporated into liposomes as previously described.^{23,25} The dry lipids of ligand (5.5 μmol), egg lecithin (20 mg; Avanti Co., 20 mL/mL in chloroform), and cholesterol (2 mg) (molar ratio 1.15:1) were suspended in 4 mL of buffer solution containing 0.9% saline and 20 mM HEPES (pH 7.4), and the resulting suspension was sonicated using a Branson ultrasonic device (model B-5200R-4) for 3 h at 4 °C. A 5-μmol amount of GdCl₃ solution from GdCl₃ stock solution was added with fast vortexing to the prepared vesicles, and sonication was continued further for 4 h. The pH was adjusted to 7.4, and the final volume was brought to 5 mL affording a 1 mM solution of gadolinium complexes used for the relaxivity measurement. The liposomal gadolinium complex of each ligand was dialyzed at 4 °C for 24 h against a saline solution (pH 7.4) that contained 0.9 wt % NaCl, 20 mM HEPES buffer, and 0.5 wt % Chelex-100 (Bio-Rad) to remove any weakly bound Gd³⁺ ions. The final liposomal Gd³⁺ concentration was typically in the 12–15 mM range.²⁶

Water-soluble Gd(ABE-DTTA): A 50-μmol portion of Gd(ABE-DTTA) per 1 kg weight of animal was prepared at 10 mM concentration and pH 7.0. A 1.2-fold excess of the ligand ABE-DTTA, compared to gadolinium, was used to prepare the complex Gd(ABE-DTTA). The dose of Gd(ABE-DTTA) (50 μmol/kg) and the sample concentration (10 mM) were calculated based on the amount of gadolinium. This formulation also contains a (1:1) Ca(ABE-DTTA) complex present at 5 mM. Thus, in the final solution, the ligand ABE-DTTA is present at a 1.7-fold excess compared to gadolinium.

For a 18.9-kg dog, the formulation was prepared as follows: A 0.412-g portion (0.68 mmol) of ABE-DTTA was dissolved in 13.6 mL of sodium hydroxide solution (0.1 N); 0.590 mL (0.567 mmol) of gadolinium chloride stock solution (0.96 M) was added in portions. The pH was repeatedly adjusted to 6.8 using NaOH (0.1 N). On the other hand, 0.1718 g (0.284 mmol) of ABE-DTTA was dissolved in 5.67 mL of NaOH (0.1 N), and 2.835 mL (0.284 mmol) of a calcium chloride solution (0.1 M) was added. The two solutions were then mixed. The pH was adjusted to 7 and the final volume to 56.7 mL (10 mM gadolinium). The solution was filtered through a 0.1-μm pore size filter, and the relaxivity was measured.

Acknowledgment. Parts of this work were supported by NIH Grant RO1 HL51146 (G.A.E.). The excellent technical assistance of Marina Mazur and Ling-Ling Guo is greatly appreciated. We are also grateful to Dr. Wen Jang Chu for several of our relaxivity determinations.

References

- Gotto, A. M.; Farmer, J. A. Risk Factors for Coronary Artery Disease. In *Heart Disease: A Textbook of Cardiovascular Medicine*; Braunwald, E., Ed.; WB Saunders: Philadelphia, PA, 1988; p 1153.
- de Roos, A.; van der Wall, E. E.; Burschke, A. V.; van Voorthuisen, A. E. Magnetic Resonance Imaging in the Diagnosis and Evaluation of Myocardial Infarction. *Magn. Reson. Q.* 1992, 7, 191–207.
- Budinger, T. F. NMR in Vivo Studies; Comparison with Other Noninvasive Imaging Techniques. In *Nuclear Magnetic Resonance (NMR) Imaging*; Partain, C. L., James, A. E., Jr., Rollo, F. D., Price, R. R., Eds.; WB Saunders: Philadelphia, PA, 1983; pp 357–374.
- Lauterbur, P. C. Image Formation by Induced Local Interactions: Examples Employing Nuclear Magnetic Resonance. *Clin. Orthop. Related Res.* 1973, 244, 3–6.
- Bakal, C. A.; Strauss, H. W. Radionuclide Imaging. In *Noninvasive Cardiac Imaging*; Morganroth, J., Parisi, A. F., Pohost, G. E., Eds.; Year Book Medical Publishers Inc.; Chicago, London, 1983; pp 21–52.
- Cooke, P.; Morris, P. G. The effects of NMR exposure on living organisms. II. A Genetic Study of Human Lymphocytes. *Br. J. Radiol.* 1981, 54, 622–625.
- Canby, R. C.; Elgavish, G. A.; Pohost, G. M. Paramagnetic NMR Contrast Agents for Cardiovascular Imaging. In *New Concepts Cardiac Imaging*; Pohost, G. M., Ed.; Yearbook Medical Publishers Inc.: Chicago, London, 1987; pp 315–342.
- Reuben, J.; Elgavish, G. A. Shift Reagents and the NMR of Paramagnetic Lanthanide Complexes. In *Handbook on the Physics and Chemistry of Rare Earths*; Gschneider, K. A., Jr., Eyring, L., Eds.; North-Holland Publishing Co.: Amsterdam, New York, Oxford, 1979; Vol. 4, pp 483–514.
- Degani, H.; Elgavish, G. A. Ionic Permeabilities of Membranes: ²³Na and ⁷Li NMR Studies of ion Transport across the Membrane of Phosphatidylcholine Vesicles. *FEBS Lett.* 1978, 90, 357–360.
- Reuben, J. Bioinorganic Chemistry: Lanthanides as Probes in Systems of Biological Interest. In *Handbook on the Physics and Chemistry of Rare Earths*; Gschneider, K. A., Jr., Eyring, L., Eds.; North-Holland Publishing Co.: Amsterdam, New York, Oxford, 1979; Vol. 4, pp 515–585.
- Carr, D. H.; Brown, J.; Bydder, G. M.; Steiner, R. E.; Weinmann, H. J.; Speck, U.; Hall, A. S.; Young, I. R. Gadolinium-DTPA as a Contrast Agent in MRI: Initial Clinical Experience in 20 Patients. *Am. J. Roent.* 1984, 143 (2), 215–224.
- Lauffer, R. B. Paramagnetic Metal Complexes as Water Proton Relaxation Agents for NMR Imaging: Theory and Design. *Chem. Rev.* 1987, 87, 901–927.
- Runge, V. M.; Claussen, C.; Felix, R.; James, A. E., Jr., Eds. *Contrast Agents in Magnetic Resonance Imaging*; Excerpta Medica: Princeton, NJ, 1986.
- Van Wagoner, M.; O'Toole, M.; Worah, D.; Leese, P. T.; Quay, S. C. A Phase I Clinical Trial with Gadolinium Injection, a Nonionic Magnetic Resonance Imaging Enhancement Agent. *Invest. Radiol.* 1991, 26, 980–986.
- Runge, V. M.; Bronen, R. A.; Davis, K. R. Efficacy of Gadoteridol for Magnetic Resonance Imaging of the Brain and Spine. *Invest. Radiol.* 1992, 27 (1), S22–S32.
- Wolf, G. L.; Fobben, E. S. The Tissue Proton T1 and T2 Response to Gadolinium DTPA Injection in Rabbits. A Potential Renal Contrast Agent for NMR Imaging. *Invest. Radiol.* 1984, 19, 324–328.

- (17) Saeed, M.; Wendland, M. F.; Tomei, E.; Rocklage, S. N.; Quay, S. C.; Moseley, M. E.; Wolfe, C.; Higgins, C. B. Demarcation of Myocardial Ischemia: Magnetic Susceptibility Effect of Contrast Medium in MR Imaging. *Radiology* **1989**, *173* (3), 763-767.
- (18) Kang, S. I.; Ranganathan, R. S.; Emswiler, J. E.; Kumar, K.; Gougoutas, J. Z.; Malley, M. F.; Tweedle, M. F. Synthesis, Characterization, and Crystal Structure of the Gadolinium (III) Chelate of (1R,4R,7R)- α,α',α'' -trimethyl-1,4,7,10-tetraazacycododecane-1,4,7-triacetic acid (DO3MA). *Inorg. Chem.* **1993**, *32*, 2912-2918.
- (19) Lauffer, R. B.; Brady, T. J.; Brown, R. D.; Baglin, C.; Koenig, S. H. $1/T_1$ NMRD Profiles of Solutions of Mn^{2+} and Gd^{3+} Protein-Chelate Conjugates. *Magn. Reson. Med.* **1986**, *3* (4), 541-548.
- (20) Evans, J. R.; Gunton, R. W.; Baker, R. G. Use of Radioiodinated Fatty Acid for Photoscans of the Heart. *Circ. Res.* **1965**, *16*, 1-10.
- (21) Bonte, F. J.; Graham, K. D.; Moore, J. G. Experimental Myocardial Imaging with ^{131}I -labeled Oleic Acid. *Radiology* **1973**, *108*, 195-196.
- (22) Kim, S. K.; Pohost, G. M.; Elgavish, G. A. Fatty Acyl Iminopolycarboxylates: Lipophilic Bifunctional Contrast Agents for NMR Imaging. *Magn. Reson. Med.* **1991**, *22*, 57-67.
- (23) Kim, S. K.; Pohost, G. M.; Elgavish, G. A. Gadolinium Complexes of [(Myristoryloxy)propyl] diethylenetriaminetetraacetate: New Lipophilic, Fatty Acyl Conjugated NMR Contrast Agents. *Bioconjugate Chem.* **1992**, *3* (1), 20-26.
- (24) Simor, T.; Chu, W.-J.; Johnson, L.; Safranko, A.; Doyle, M.; Pohost, G. M.; Elgavish, G. A. In vivo MRI Visualization of Acute Myocardial Ischemia and Reperfusion in Ferrets by the Persistent Action of the Contrast Agent Gd(BME-DTTA). *Circulation* **1995**, *92* (12), 3549-3559.
- (25) Chu, W.-J.; Simor, T.; Elgavish, G. A. In vivo Characterization of Gd(BME-DTTA), a Myocardial MRI Contrast Agent: Tissue Distribution of its MRI Intensity Enhancement and its Effect on Heart Function. *NMR Biomed.* **1997**, *10*, 87-92.
- (26) Koenig, S. H.; Baglin, C.; Brown, R. D., III; Brewer, C. F. Magnetic Field Dependence of Solvent Proton Relaxation Induced by Gd^{3+} and Mn^{2+} Complexes. *Magn. Reson. Med.* **1984**, *1* (4), 496-501.
- (27) Larrabee, A. L. Time-dependent Changes in the Size Distribution of Distearoyl Phosphatidylcholine Vesicles. *Biochemistry* **1979**, *18* (15), 3321-3326.
- (28) Weinmann, H. J.; Grier, H. Paramagnetic Contrast Media in NMR Tomography-Basic Properties and Experimental Studies in Animals. *Magn. Reson. Med.* **1984**, *1*, 271-272.

JM980454V